

Scaling of temporal correlations in an attractive Tomonaga-Luttinger spin liquid

K. Yu. Povarov,¹ D. Schmidiger,¹ N. Reynolds,¹ R. Bewley,² and A. Zheludev¹

¹*Neutron Scattering and Magnetism, Laboratory for Solid State Physics, ETH Zürich, Switzerland*

²*ISIS Facility, Rutherford Appleton Laboratory, Chilton, Didcot, Oxon OX11 0QX, United Kingdom*
(Dated: January 15, 2015)

We report temperature-dependent neutron scattering measurements of the local dynamic structure factor in the quantum spin ladder $(\text{C}_7\text{H}_{10}\text{N})_2\text{CuBr}_4$ in a magnetic field $H = 9$ T, in its gapless quantum-critical phase. We show that the measured quantity has a scaling form consistent with expectations for a Tomonaga-Luttinger liquid with attraction. The measured Luttinger parameter $K \approx 1.25$ and scaling function are in excellent agreement with density matrix renormalization group numerical calculations for the underlying spin Hamiltonian.

PACS numbers: 75.10.Kt, 75.10.Jm, 75.40.Gb, 78.70.Nx

Landau's Fermi liquid theory is the basis of our understanding of interacting fermions, be it metals or neutron stars [1–4]. Landau's main argument regarding the stability of quasiparticles breaks down in low dimensions. Interestingly, in one dimension, interacting fermions still bear a unified description, known as the Tomonaga-Luttinger liquid (TLL) [5–8]. All low-energy properties of such fermions, including thermodynamics, correlation functions, susceptibilities, etc., are predicted to be *universal* in that any details of the interaction potential are irrelevant. Instead, the interactions are characterized by a single dimensionless quantity, known as the Luttinger parameter K . Free fermions correspond to $K = 1$, $K < 1$ implies repulsive interactions, and fermions with attraction have $K > 1$.

Experimental validations of this astonishingly strong statement of universality are of utmost importance. The most obvious model systems are one-dimensional metals in charge-transfer salts [9], quantum wires [10], and quantum Hall effect edge states [11–13]. However, TLLs with the most experimentally accessible correlation functions are found in seemingly unlikely places, namely, in magnetic insulators. Following Haldane's application of the TLL description to $S = 1/2$ spin chains [14], it was realized that a great variety of one-dimensional quantum magnets fall into this universality class. The benefit of such mapping is that spin correlations can be directly probed with neutron scattering, nuclear magnetic resonance (NMR), electron spin resonance (ESR) and other techniques. A huge success of this approach was measurements of universal finite-temperature scaling laws for correlation functions in Heisenberg $S = 1/2$ chains [15 and 16]. Similar work was done on non-TLL critical systems, such as gapless spin ladders with cyclic exchange [17]. However, Heisenberg spin chains are but a very particular case of a *repulsive* TLL, with $K = 1/2$ [8 and 18]. Fermions (electrons) in quantum wires and one-dimensional metals are usually also repulsive. Very recently, it was shown that an *attractive* TLL, previously only known in certain quantum Hall edge states [13], can also be realized in magnetized $S = 1/2$ antiferromagnetic (AF) Heisenberg spin ladders [19 and 20]. NMR experiments on a prototypical ladder compound confirmed this

result [21]. However, those studies covered less than an order of magnitude in temperature at a single measurement frequency, which is insufficient to establish power law scaling and universality. In contrast, in the present Rapid Communication we use neutron spectroscopy to observe power law scaling of local temporal correlations in the same material over more than two decades in ω/T . Specifically, we find that the measured scaled local dynamic structure factor $T^{1/2K-1}\mathcal{S}(\omega)$ is a *universal* function of ω/T in wide temperature and energy ranges with $K > 1$.

The spin Hamiltonian for the AF Heisenberg spin ladder is written as:

$$\hat{\mathcal{H}} = \sum_j [J_{\parallel} \mathbf{S}_{1,j} \mathbf{S}_{1,j+1} + J_{\parallel} \mathbf{S}_{2,j} \mathbf{S}_{2,j+1} + J_{\perp} \mathbf{S}_{1,j} \mathbf{S}_{2,j}], \quad (1)$$

where $J_{\parallel} > 0$ and $J_{\perp} > 0$ are exchange constants for the ladder legs 1 and 2, and rungs, respectively. In zero magnetic field, the ground state is a non-magnetic singlet and the excitation spectrum is gapped. However, applying a magnetic field drives this gap to zero at some critical field H_{c1} by virtue of the Zeeman effect, and produces a continuum of gapless TLL states for $H > H_{c1}$. The Luttinger parameter can be continuously tuned by varying the field strength [8]. For $H \rightarrow H_{c1}$, $K \rightarrow 1$ in all cases. For $J_{\parallel} \ll J_{\perp}$, the quasiparticles can be envisioned as single-rung singlet-triplet excitations. These have hard-core like repulsion, since no rung can be excited twice. As a result, $K < 1$ for $H > H_{c1}$ [22]. However, if the leg interactions are dominant, $J_{\parallel} > J_{\perp}$, the quasiparticles are more extended in nature. For this case, numerical calculations show $K > 1$ above the critical field [20].

Our target material, $(\text{C}_7\text{H}_{10}\text{N})_2\text{CuBr}_4$, bis(2,3-dimethylpyridinium) tetrabromocuprate or DIMPY for short, is arguably the best known realization of the AF $S = 1/2$ Heisenberg ladder model [20, 23–25]. The magnetic properties are due to Cu^{2+} cations linked in ladder structures by superexchange pathways via Br^- anions (for a schematic depiction of the crystal structure see Fig. 1 in Ref. 24). Organic ligands act as spacers between these ladders in the monoclinic crystal structure, providing excellent one-dimensionality. The spin Hamil-

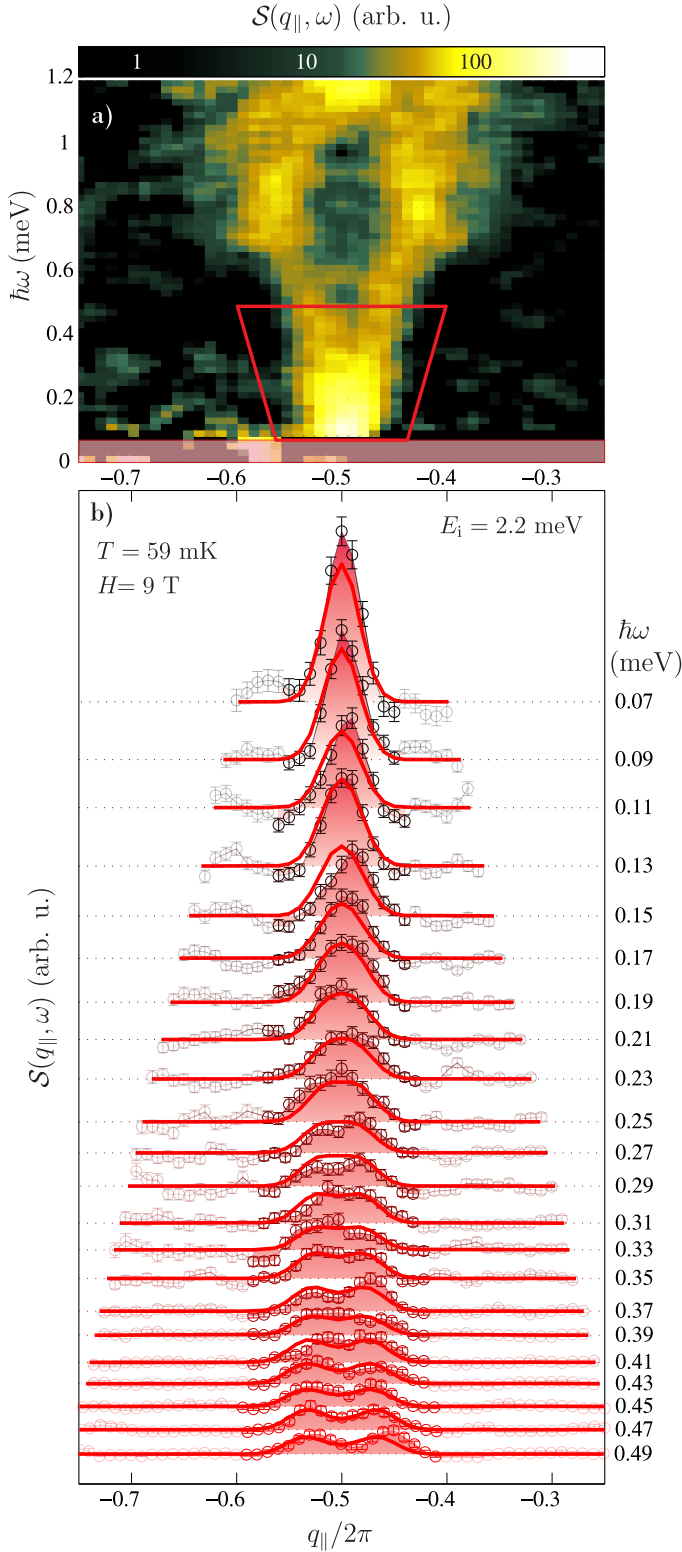


FIG. 1. (Color online) Dynamic spin structure factor of DIMPY at $T = 59$ mK, extracted from inelastic neutron intensities. (a) False color map of $S(q_{\parallel}, \omega)$. The boundary shows the region in energy-momentum space, used in the analysis. (b) Constant energy cuts with the q_{\parallel} integration range highlighted. All the data are background corrected, as described in the text. Solid lines correspond to the TLL theoretical prediction convoluted with the spectrometer resolution.

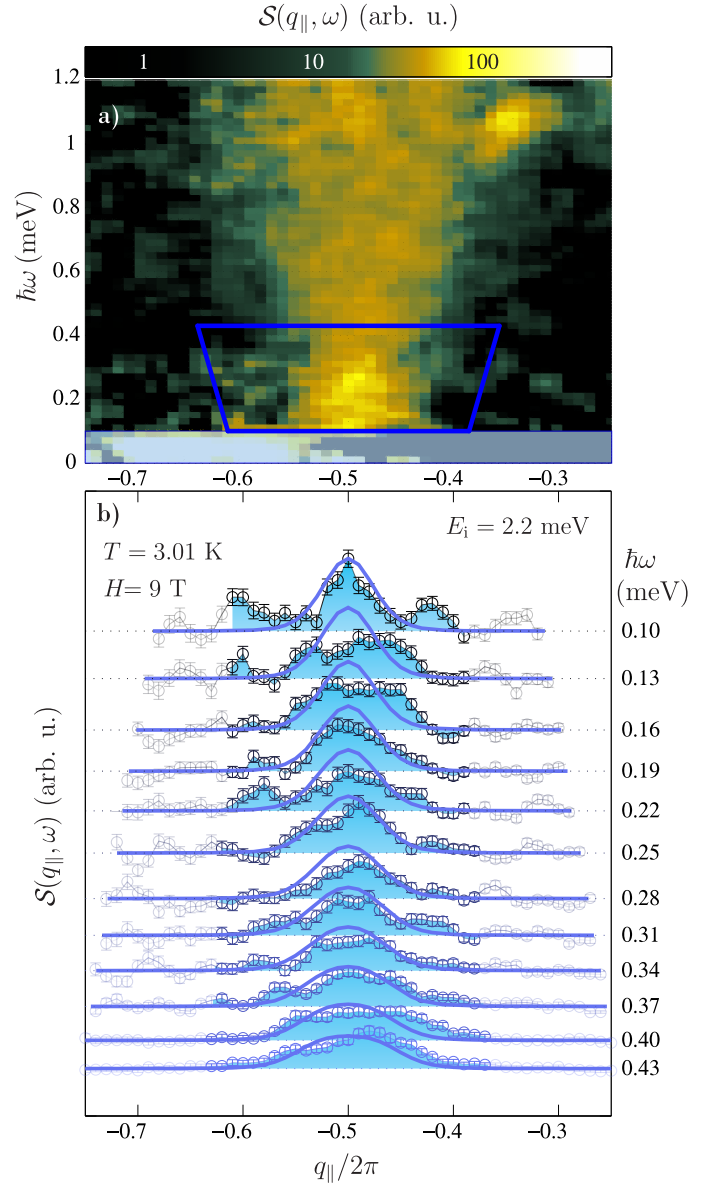


FIG. 2. (Color online) As Fig. 1, for $T = 3.01$ K.

tonian of DIMPY is well established through a quantitative comparison of inelastic neutron scattering spectra and thermodynamic data to density matrix renormalization group (DMRG) numerical calculations [24 and 25]. The two ladder exchange constants are $J_{\parallel} = 1.42$ meV and $J_{\perp} = 0.82$ meV, respectively. Interladder interactions are as small as $J' \simeq 6 \mu\text{eV}$ [20]. The ground state is a spin singlet with a gap $\Delta = 0.33$ meV. In DIMPY, the spin gap closes at $H_{c1} \simeq 2.6$ T [20, 21, and 26].

Measuring those temporal correlations in DIMPY that are relevant to TLL physics is far from straightforward. Most of the observable spectral features are specific to spin ladder physics and are not related to TLL dynamics [26]. TLL excitations are revealed only at the lowest

energies, and are barely discernible in previous measurements due to limited energy resolution. Therefore, our present experiments, while using the same sample²⁷ and the LET neutron spectrometer [28] at ISIS as in previous studies [26], took advantage of a different instrument configuration with a lower neutron incident energy $E_i = 2.2$ meV. This allowed us to achieve a calculated energy resolution of $\delta E \sim 20 - 30$ μ eV, depending on energy transfer.

Neutron experiments are used to determine the dynamic structure factors $\mathcal{S}^{\alpha\alpha}(\mathbf{Q}, \omega)$ as a function of momentum transfer \mathbf{Q} and energy transfer $\hbar\omega$. For each spin component α , these quantities are a Fourier transform of the spin correlation functions of interest: $\mathcal{S}^{\alpha\alpha}(\mathbf{Q}, \omega) = \int e^{-i((\mathbf{Q}\cdot\mathbf{r})-\omega t)} \langle S^\alpha(0,0)S^\alpha(\mathbf{r},t) \rangle d\mathbf{r}dt$. In practice, one measures the neutron partial differential cross-section, which in our case is proportional to the sum of structure factors for spin components parallel and perpendicular to the applied field: $\mathcal{S}(\mathbf{Q}, \omega) = \mathcal{S}^{zz}(\mathbf{Q}, \omega) + \mathcal{S}^{\perp\perp}(\mathbf{Q}, \omega)$ [29].

The thus-defined structure factor $\mathcal{S}(\mathbf{Q}, \omega)$, measured at $H = 9$ T and $T = 59$ mK, is shown in Fig. 1a. Here and below, it is plotted as a function of $q_{\parallel} = (\mathbf{Q} \cdot \mathbf{a})$, where the a crystallographic axis is along the ladder direction. Previous DMRG calculations identified all the main components of the excitation spectrum [26]. Thus, we know that the prominent gapped incommensurate excitations seen at $H = 9$ T at around ≈ 0.8 meV energy transfer are due to longitudinal spin correlations $\mathcal{S}^{zz}(q_{\parallel}, \omega)$ and are not TLL related. Since they can not be avoided in the experiment, our analysis only considers the data below $\hbar\omega = 0.5$ meV. Here it is due to correlations between transverse spin components, so $\mathcal{S}(q_{\parallel}, \omega) \simeq \mathcal{S}^{\perp\perp}(q_{\parallel}, \omega)$. The latter is representative of TLL correlations, and is the main focus of this study. The scattering at these low energies is a V-shaped continuum visible in Fig. 1(a) around the commensurate point $q_{\parallel} = -\pi$. The slope of the lower bound of the observed continuum, discernible as the separation between the two separate peaks seen at higher energies in Fig. 1, corresponds to the Fermi velocity of the TLL. Since q_{\parallel} is dimensionless in our notation, for consistency the velocity is measured in energy units, so that $\hbar\omega = uq_{\parallel}$ for a linear dispersion relation. The experimental value $u = 1.98 \pm 0.02$ meV is in excellent agreement with the DMRG result $u = 1.91$ meV for DIMPY at $H = 9$ T [20].

Having chosen a suitable measurement window, we still need to ensure that the TLL mapping remains valid in that range. The essences of the TLL model are (i) a linear dispersion relation for the fermions and (ii) an infinitely deep Fermi sea. It is a valid approximation only if the experimental energy transfers and temperature do not probe the actual Fermi sea too deeply or extend to non-linear dispersion regimes. Looking at previous DMRG calculations for $\mathcal{S}^{\perp\perp}(q_{\parallel}, \omega)$ at a similar field $H = 7$ T, we conclude that in our case (i) holds to at least 1 meV energy transfer. At $H = 9$ T the depth of the Fermi sea is $\Delta_F = g\mu_B(H - H_{c1}) \sim 0.77$ meV. Since we have already limited ourselves to excitations below 0.5 meV, the TLL

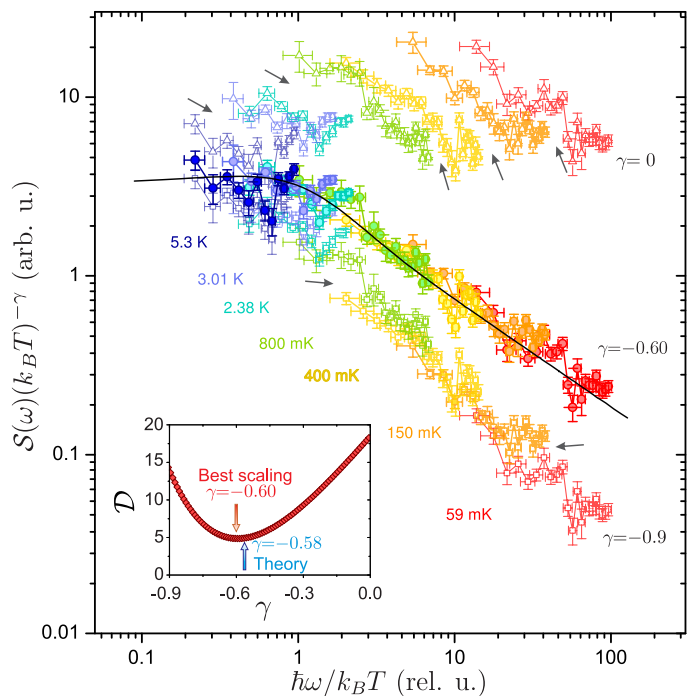


FIG. 3. (Color) Local dynamic structure factor $\mathcal{S}(\omega)$ measured in DIMPY at $H = 9$ T at several temperatures, plotted in the scaling representation with different scaling exponents γ . Arrows mark the apparent violations of scaling for non-optimal values of γ . The solid line is the exact TLL scaling function F [Eq. (2)] with the Luttinger parameter $K = 1.25$, corresponding to $\gamma = -0.6$. Inset: γ dependence of data overlap function \mathcal{D} [Eq. (3)].

model should be applicable with a good safety margin, as long as we also limit the experimental temperatures to $T < 5$ K ~ 0.5 meV/ k_B .

Constant-energy cuts from two data sets collected at the base temperature and at $T = 3$ K are shown in Figs. 1(b) and 2(b), respectively. Here the background, measured in zero applied field at the base temperature, as described in Ref. 26, was subtracted. At $H = 9$ T, the finite momentum resolution of our experiments prevents us from discerning any internal structure of the excitation continuum below 0.25 meV. As was done previously for $S = 1/2$ chain systems [15, 30, and 31], this problem was entirely avoided by integrating the dynamic structure factor over q_{\parallel} . The integration range was limited to the trapezoidal areas indicated in Figs. 1(a) and 2(a), to avoid picking up additional noise. The resulting momentum-integrated structure factor is the local temporal transverse spin correlation function in frequency representation $\mathcal{S}^{\perp\perp}(\omega)$.

We chose to analyze these data in two separate stages. First, we consider the temperature dependence of the measured structure factor without referring to specific results for the TLL. In fact, our only starting consideration is that the magnetized spin ladder is in a quantum-critical

state [32], and that $\mathcal{S}^{\perp\perp}(\omega)$ is precisely the critical correlation function. In this case, the only relevant energy scale is temperature itself, so that the *shape* of $\mathcal{S}^{\perp\perp}(\omega)$ is a function of a single variable of ω/T . One can then expect the following scaling form for this quantity [33]:

$$\mathcal{S}^{\perp\perp}(\omega) = (k_B T)^\gamma F(\hbar\omega/k_B T). \quad (2)$$

If so, with an appropriate choice of the scaling exponent γ , we should observe a data collapse for measurements collected at different temperatures. For illustration purposes, Fig. 3a shows scaling plots of our data obtained with three different exponents. For $\gamma = 0$ and $\gamma = -0.9$ the data collapse is visually less than perfect, with discontinuities indicated by arrows. For a more meaningful discussion, though, we introduced an *ad hoc* measure of the quality of the data overlap,

$$\mathcal{D} = \sum_{n,i,j} \frac{(\sigma_{n,i} - \sigma_{n+1,j})^2}{(\Delta\sigma_{n,i} + \Delta\sigma_{n+1,j})^2} \frac{1}{\sum_{n,i,j}}, \quad (3)$$

where $\sigma_{n,i} = \mathcal{S}(\omega_{ni})|_{T=T_n}/(k_B T_n)^\gamma$, i, j enumerate the nearest-neighbor pairs of points in data subsets T_n and T_{n+1} , and $\Delta\sigma_{n,i}$ is the corresponding error. The inset of Fig. 3 shows the γ dependence of \mathcal{D} . The thus defined data overlap is optimized with $\gamma = -0.60$, where \mathcal{D} has a minimum, as indicated by the arrow in the inset of Fig. 3. The corresponding scaling plot of $\mathcal{S}(\omega)$ is shown as solid symbols in the main panel Fig. 3. An excellent overlap between data sets collected at different temperatures is apparent.

Having experimentally established the scaling form of the local dynamic structure factor, we can compare the result to predictions of TLL theory. In this model the dynamic structure factor scales with a known scaling function and exponent [8 and 33]:

$$\begin{aligned} \mathcal{S}^{\perp\perp}(q_{\parallel}, \omega) &\propto T^{1/2K-2} \times \\ &\times \Im \left\{ \left[1 - \exp\left(-\frac{\hbar\omega}{k_B T}\right) \right]^{-1} \Phi\left(\frac{\hbar\omega}{k_B T}, \frac{u(q_{\parallel} - \pi)}{k_B T}\right) \right\}, \\ \Phi(x, y) &= \frac{\Gamma(\frac{1}{8K} - i\frac{x-y}{4\pi})}{\Gamma(1 - \frac{1}{8K} - i\frac{x-y}{4\pi})} \frac{\Gamma(\frac{1}{8K} - i\frac{x+y}{4\pi})}{\Gamma(1 - \frac{1}{8K} - i\frac{x+y}{4\pi})}. \end{aligned} \quad (4)$$

Integrating over momentum and comparing this to Eq. 2 yields $\gamma = \frac{1}{2K} - 1$. From the experimentally determined scaling exponent γ we then get $K \approx 1.25$. Thus,

we are dealing with one-dimensional fermions *with attraction*: $K > 1$. The comparison with TLL theory can be taken further. By numerically integrating the function Φ in Eq. 4, using $K = 1.25$ and an arbitrary overall scale factor, we get the solid line shown in Fig. 3 to illustrate the excellent agreement between experiment and the TLL model. Our precise understanding of the spin Hamiltonian for DIMPY allows us to make a direct comparison of our experimental findings to numerical calculations. Using the field dependence of the Luttinger parameter previously calculated for DIMPY using DMRG [20], for $H = 9$ T we get $K = 1.20$ or, equivalently, $\gamma = -0.58$. This numerically obtained scaling exponent is, to within experimental error, indistinguishable from our *ad hoc* experimental value, and the data collapse is almost as good. Equation (4) can now be used to model the entire energy- and wavevector-dependent scattering intensity measured in our experiments. Numerically convoluting the analytical expression with the calculated spectrometer resolution, we get constant-energy cuts shown in solid lines in Figs. 1(b) and 2(b). Note that the only adjustable parameter in this fit is a single overall scaling factor for all temperatures and energies. Considering the experimental noise and systematic errors due to background subtraction, the level of agreement with experiment is excellent.

In summary, we show that the local dynamic structure factor for a magnetized strong-leg quantum spin ladder has a finite-temperature scaling form expected for a quantum-critical system. The experimentally determined scaling exponent and scaling function are in excellent agreement with those for an *attractive* Tomonaga-Luttinger liquid. In fact, the results are fully consistent with numerical calculations for the particular model spin Hamiltonian of the target compound. We would like to emphasize that neutron scattering experiments with energy resolution, intensity, and signal-to-background ratios necessary for such studies were enabled only very recently by major breakthroughs in neutron instrumentation at user facilities such as ISIS.

This work was supported by the Swiss National Science Foundation, Division 2. We would like to thank S. Mühlbauer (FRM II, Technische Universität München) for his involvement in the early stages of this project. A. Z. would like to thank Professor T. Giamarchi and Professor F. H. L. Essler for numerous enlightening discussions on the subject of critical dynamics.

¹ L. D. Landau, “The theory of a Fermi liquid,” Sov. Phys. - JETP **3**, 920–925 (1957).

² L. D. Landau, “On the theory of a Fermi liquid,” Sov. Phys. - JETP **8**, 70 (1959).

³ E. M. Lifshitz and L. P. Pitaevskii, *Statistical Physics: Theory of the Condensed State* (Elsevier, Amsterdam, 1980).

⁴ A. A. Abrikosov, *Fundamentals of the Theory of Metals* (North-Holland, Amsterdam, 1988).

⁵ S. Tomonaga, “Remarks on Bloch’s method of sound waves applied to many-fermion problems,” Prog. Theor. Phys. **5**, 544–569 (1950).

⁶ J. M. Luttinger, “An exactly soluble model of a many-fermion system,” J. Math. Phys. **4**, 1154–1162 (1963).

- ⁷ D. C. Mattis and E. H. Lieb, “Exact solution of a many-fermion system and its associated boson field,” *J. Math. Phys.* **6**, 304–312 (1965).
- ⁸ T. Giamarchi, *Quantum Physics in One Dimension* (Clarendon, Oxford U.K., 2004).
- ⁹ F. Zwick, S. Brown, G. Margaritondo, C. Merlic, M. Onellion, J. Voit, and M. Grioni, “Absence of quasiparticles in the photoemission spectra of quasi-one-dimensional Bechgaard salts,” *Phys. Rev. Lett.* **79**, 3982–3985 (1997).
- ¹⁰ A. Yacoby, H. L. Stormer, Ned S. Wingreen, L. N. Pfeiffer, K. W. Baldwin, and K. W. West, “Nonuniversal conductance quantization in quantum wires,” *Phys. Rev. Lett.* **77**, 4612–4615 (1996).
- ¹¹ A. M. Chang, L. N. Pfeiffer, and K. W. West, “Observation of chiral Luttinger behavior in electron tunneling into fractional quantum Hall edges,” *Phys. Rev. Lett.* **77**, 2538–2541 (1996).
- ¹² M. Grayson, D. C. Tsui, L. N. Pfeiffer, K. W. West, and A. M. Chang, “Continuum of chiral Luttinger liquids at the fractional quantum Hall edge,” *Phys. Rev. Lett.* **80**, 1062–1065 (1998).
- ¹³ M. Grayson, L. Steinke, D. Schuh, M. Bichler, L. Hoeppe, J. Smet, K. v. Klitzing, D. K. Maude, and G. Abstreiter, “Metallic and insulating states at a bent quantum Hall junction,” *Phys. Rev. B* **76**, 201304 (2007).
- ¹⁴ F. D. M. Haldane, “General relation of correlation exponents and spectral properties of one-dimensional fermi systems: Application to the anisotropic $S = 1/2$ Heisenberg chain,” *Phys. Rev. Lett.* **45**, 1358–1362 (1980).
- ¹⁵ D. C. Dender, Ph.D. thesis, Johns Hopkins University, 1997.
- ¹⁶ B. Lake, D. A. Tennant, C. D. Frost, and S. E. Nagler, “Quantum criticality and universal scaling of a quantum antiferromagnet,” *Nat. Mater.* **4**, 329–34 (2005).
- ¹⁷ B. Lake, A. M. Tsvelik, S. Notbohm, D. A. Tennant, T. G. Perring, M. Reehuis, C. Sekar, G. Krabbes, and B. Büchner, “Confinement of fractional quantum number particles in a condensed-matter system,” *Nat. Phys.* **6**, 50–55 (2010).
- ¹⁸ H. J. Schulz, “Phase diagrams and correlation exponents for quantum spin chains of arbitrary spin quantum number,” *Phys. Rev. B* **34**, 6372–6385 (1986).
- ¹⁹ T. Hikiyara and A. Furusaki, “Spin correlations in the two-leg antiferromagnetic ladder in a magnetic field,” *Phys. Rev. B* **63**, 134438 (2001).
- ²⁰ D. Schmidiger, P. Bouillot, S. Mühlbauer, S. Gvasaliya, C. Kollath, T. Giamarchi, and A. Zheludev, “Spectral and thermodynamic properties of a strong-leg quantum spin ladder,” *Phys. Rev. Lett.* **108**, 167201 (2012).
- ²¹ M. Jeong, H. Mayaffre, C. Berthier, D. Schmidiger, A. Zheludev, and M. Horvatić, “Attractive Tomonaga-Luttinger liquid in a quantum spin ladder,” *Phys. Rev. Lett.* **111**, 106404 (2013).
- ²² P. Bouillot, C. Kollath, A. M. Läuchli, M. Zvonarev, B. Thielemann, C. Rüegg, E. Orignac, R. Citro, M. Klanjšek, C. Berthier, M. Horvatić, and T. Giamarchi, “Statics and dynamics of weakly coupled antiferromagnetic spin- $\frac{1}{2}$ ladders in a magnetic field,” *Phys. Rev. B* **83**, 054407 (2011).
- ²³ T. Hong, Y. H. Kim, C. Hotta, Y. Takano, G. Tremelling, M. M. Turnbull, C. P. Landee, H.-J. Kang, N. B. Christensen, K. Lefmann, K. P. Schmidt, G. S. Uhrig, and C. Broholm, “Field-induced Tomonaga-Luttinger liquid phase of a two-leg spin-1/2 ladder with strong leg interactions,” *Phys. Rev. Lett.* **105**, 137207 (2010).
- ²⁴ D. Schmidiger, S. Mühlbauer, S. N. Gvasaliya, T. Yankova, and A. Zheludev, “Long-lived magnons throughout the Brillouin zone of the strong-leg spin ladder $(\text{C}_7\text{H}_{10}\text{N})_2\text{CuBr}_4$,” *Phys. Rev. B* **84**, 144421 (2011).
- ²⁵ D. Schmidiger, P. Bouillot, T. Guidi, R. Bewley, C. Kollath, T. Giamarchi, and A. Zheludev, “Spectrum of a magnetized strong-leg quantum spin ladder,” *Phys. Rev. Lett.* **111**, 107202 (2013).
- ²⁶ D. Schmidiger, S. Mühlbauer, A. Zheludev, P. Bouillot, T. Giamarchi, C. Kollath, G. Ehlers, and A. M. Tsvelik, “Symmetric and asymmetric excitations of a strong-leg quantum spin ladder,” *Phys. Rev. B* **88**, 094411 (2013).
- ²⁷ In all neutron experiments we used fully deuterated samples to avoid the strong incoherent scattering from H nuclei.
- ²⁸ R.I. Bewley, J.W. Taylor, and S.M. Bennington, “LET, a cold neutron multi-disk chopper spectrometer at ISIS,” *Nucl. Instrum. Methods Phys. Res., Sect. A* **637**, 128 – 134 (2011).
- ²⁹ G. L. Squires, *Introduction to the Theory of Thermal Neutron Scattering* (Cambridge University Press, Cambridge, U.K., 2012).
- ³⁰ A. Zheludev, T. Masuda, G. Dhalenne, A. Revcolevschi, C. Frost, and T. Perring, “Scaling of dynamic spin correlations in $\text{BaCu}_2(\text{Si}_{0.5}\text{Ge}_{0.5})_2\text{O}_7$,” *Phys. Rev. B* **75**, 054409 (2007).
- ³¹ G. Simutis, S. Gvasaliya, M. Månsson, A. L. Chernyshev, A. Mohan, S. Singh, C. Hess, A. T. Savici, A. I. Kolesnikov, A. Piovano, T. Perring, I. Zaliznyak, B. Büchner, and A. Zheludev, “Spin pseudogap in Ni-doped SrCuO_2 ,” *Phys. Rev. Lett.* **111**, 067204 (2013).
- ³² S. Sachdev, T. Senthil, and R. Shankar, “Finite-temperature properties of quantum antiferromagnets in a uniform magnetic field in one and two dimensions,” *Phys. Rev. B* **50**, 258–272 (1994).
- ³³ S. Sachdev, *Quantum Phase Transitions* (Cambridge University Press, Cambridge, U.K., 2011).